Chromosome Research **8**: 243–252, 2000.

Chromosome no. 1 of *Crepis capillaris* shows defined 3D-shapes in mitotic prophase

A. B. Houtsmuller[1], J. L. Oud[1], M. B. Montijn[1], M. Worring[2], A. W. M. Smeulders[2] & N. Nanninga[1]*
[1]*BioCentrum Amsterdam, Institute for Molecular Cell Biology, University of Amsterdam, The Netherlands; Tel: +31 20 525 5187; Fax: +31 20 525 6271; E-mail: nanninga@bio.uva.nl;* [2]*Faculteit voor Wiskunde en Informatica (FWI), University of Amsterdam, The Netherlands*
* *Correspondence*

Received 16 August 1999; received in revised form and accepted for publication by A. Sumner 22 December 1999

Key words: confocal microscopy, *Crepis capillaris*, plant chromosome, prophase chromosome shape

Abstract

The shape of mitotic prophase chromosomes has been studied in root tip nuclei by confocal microscopy and 3D-image analysis. *Crepis capillaris* chromosome no. 1 was used as a test object. Chromosome conformation was studied in early, mid- and in late prophase. In mid- and late prophase, individual chromosomes could be distinguished on the basis of their length. Early prophase chromosomes could not be distinguished as individuals. The central axes of prophase chromosomes were traced with an automated computer procedure and then represented as a string of 3D coordinates. This representation facilitated measurement along the chromosome axis of shape parameters such as curvature (amount of bending), torsion (helical winding) and torsion sign (helical handedness). Stretches of early prophase chromosomes showed full helical turns, which could be left- or right-handed. In the later prophase stages curvature and torsion were statistically analysed. Our data on 40 mid-prophase chromosomes no. 1 show that they are still highly curved, but full helical turns were no longer found. Instead, an overall meandering pattern was observed. In late prophase, one central loop persisted, flanked by two preferential regions of high curvature.

Introduction

Chromatin occurs at various levels of compaction during the cell cycle. Only at the nucleosome level is the structure known at atomic dimensions (Luger *et al.* 1997). With respect to higher levels of organisation, little is known, though several models have been proposed to account for chromatin folding into mitotic chromosomes (DuPraw 1966, Sedat & Manuelidis 1977, Agard & Sedat 1983, Earnshaw 1988, Belmont *et al.* 1989, Manuelidis 1990, Manuelidis & Chen 1990, Marshall *et al.* 1996). Apart from very global features, there is also hardly any knowledge about the dynamics of the 3D-folding patterns of chromosomes during condensation from prophase to metaphase.

In a conceptual and methodological pioneering study, the folding patterns of interphase polytene chromosomes in *Drosophila melanogaster* have been studied (Hochstrasser & Sedat 1987). In the present study the results of analysis of the folding pattern of the much smaller prophase chromosomes of *Crepis capillaris* are presented. *C. capillaris* was chosen because of its small number of chromosomes and because the chromosomes can be recognized by their length in mitotic cells ($2n = 6$; cf. Oud *et al.* 1989 and references therein). To study the dynamics of

contraction, prophase nuclei were divided into three subclasses: early, mid and late prophase. The axes of whole mid and late prophase chromosomes as well as parts of early chromosomes were traced with the aid a semi-automatic procedure (Houtsmuller *et al.* 1993). Chromosome no. 1, the longest, has been analysed in mid and in late prophase. As 3D-shape parameters, curvature (amount of bending) and torsion (helical winding) were measured as a function of the chromosomes' medial axes. Distinct structural features could be observed during the progression of prophase towards metaphase.

Materials and methods

Chromosome preparation

Roots were taken from *C. capillaris* plants grown for 4 weeks in a greenhouse. After harvesting, the roots were immediately fixed in modified Carnoy for at least 30 min. Root tips of approximately 5–10 mm length were rinsed in water, then hydrolysed for 5 min in 1 N HCl at 60°C and stained for 1 h in the Feulgen solution. The cells were then macerated in 45% (v/v) acetic acid and thereafter placed between two coverslips; care was taken to avoid squashing the root tissue.

3D chromosome images

3D images of prophase nuclei of *C. capillaris* root tips were obtained by confocal microscopy (for technical details, see Brakenhoff *et al.* 1990). To excite the Feulgen fluorescence, the 530.9-nm line of a krypton ion laser was used in combination with a 580-nm dichroic mirror and a 580-nm blocking filter. The prophase nuclei studied were scanned in a variable number of optical sections. Each section consisted of 256×256 pixels of 100×100 nm each. The distance between the optical sections was 400 nm. The fluorescence intensity data were stored as integers with a value between 0 and 255 in an eight-bit memory array as a function of the position in the preparation.

Analysis of 3D-coordinate strings

To obtain 3D-coordinate strings of chromosomes, their medial axes were traced in the 3D image with the aid of a semi-automatic computer algorithm (Houtsmuller *et al.* 1993). In this procedure, the user interactively indicates with a 3D cursor the beginning and end of a chromosome. After that, a path-tracing algorithm automatically steps along the chromosomal axis with equidistant steps. The points thus encountered are stored as a string of 3D coordinates (Houtsmuller *et al.* 1993).

The analysis of 3D-coordinate strings takes place in three steps. First, the tracing result is visually compared with the original image by interactive rotation, and second, the typical 3D shape parameters, curvature (amount of bending) and torsion (helical winding), are mathematically determined (see below). Statistical analysis of the curvature and torsion patterns is carried out to test the significance of observed general features.

Mathematical shape analysis

To estimate the shape of the chromosomes' medial axes, two line shape parameters, curvature and torsion, were extracted from the 3D-coordinate strings (Worring *et al.* 1994). For this purpose, approximating splines were fitted through each point along the coordinate string (Woltring 1986). Splines are analytical curves and therefore allow curvature and torsion measurement. The position along the chromosome axes of local curvature maxima and torsion-sign alternations (i.e. the changing of the torsion sign, where positive torsion reflects right-handed helical winding and negative torsion left-handed winding) were taken as descriptors of the chromosomal folding pattern.

Results

C. capillaris was chosen for the 3D shape analysis of prophase chromosomes because it has few chromosomes ($2n = 6$), and because the individual homologous pairs can be distinguished on the basis of their length from mid prophase to late anaphase (cf. Oud *et al.* 1989 and references therein). To gain insight into the dynamic process of chromosome condensation, the prophase nuclei were subdivided into three stages: early, mid and late prophase. Early prophase (Figure 1a) has been defined as the stage at which individual chromosomes are not visually distinguishable over their full

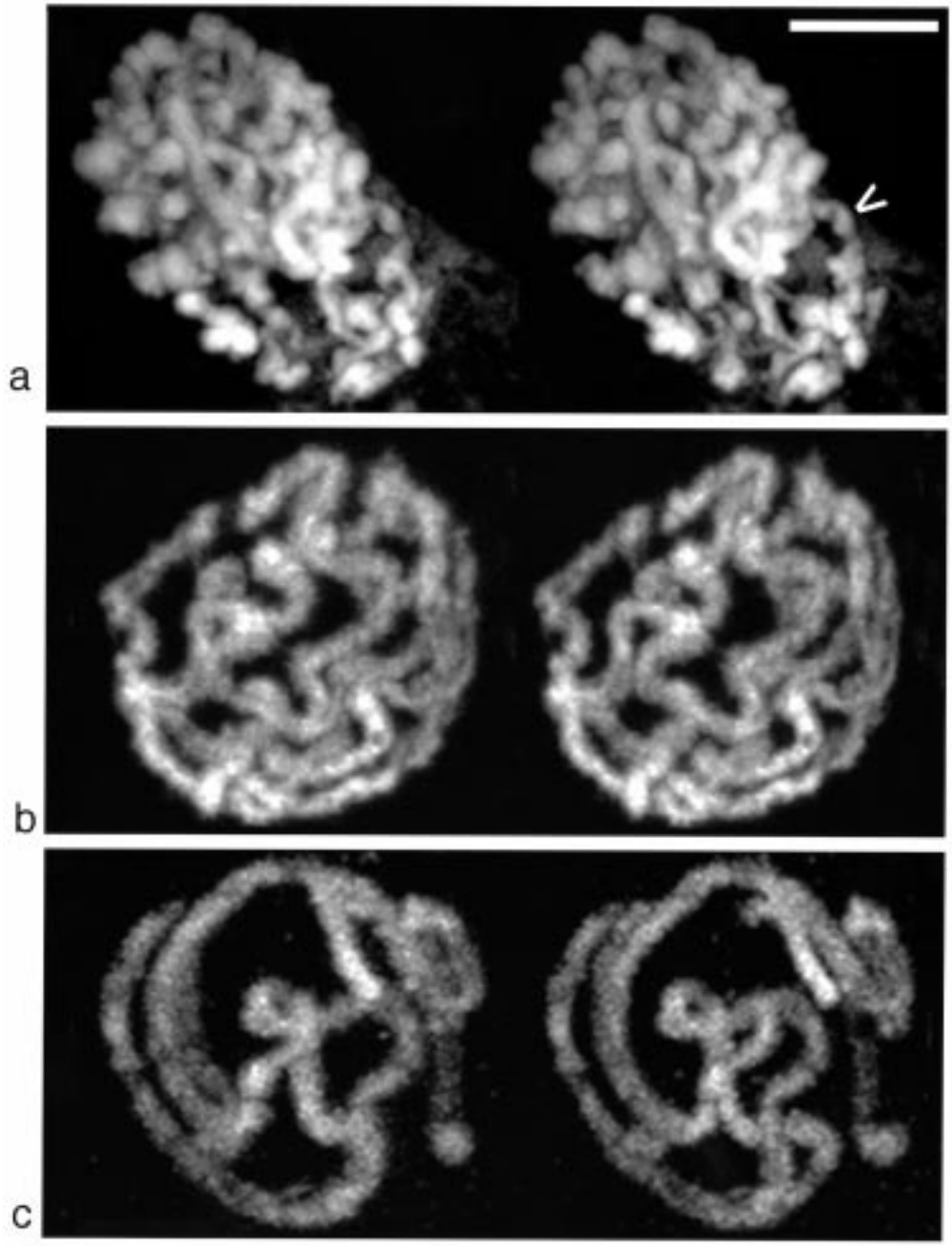

Figure 1. Stereo images (mounted for parallel viewing) of three typical examples of *Crepis capillaris* nuclei in the prophase substages. (**a**) early; (**b**) mid and (**c**), late prophase. Bar = 5 μm.

length. Nuclei were classified as mid prophase (Figure 1b) when five or six of the chromosomes were distinguishable after interactive reconstruction with the aid of the 'homing cursor' procedure (see below). A prophase was defined as late (Figure 1c) when all six chromosomes were distinguishable by visual inspection of stereo images. Because we wished to choose one particular chromosome for 3D analysis, we have focused our analysis on chromosome no. 1.

Visualization of prophase chromosomes

The 3D prophase images were studied with the aid of the visualization method used in the homing cursor program (Houtsmuller *et al.* 1993). In this program, three projections of the confocal data set are displayed simultaneously: a front view is displayed in a central box (XY projection); a top (XZ projection) and a side view (YZ projection) are displayed in the other boxes (Figure 2a). A mouse-controlled cursor (+) is placed in the 3D image and is displayed in all three views. In each box, the cursor can be moved and the cursors in the other boxes move accordingly. In addition, the user can choose in each box whether one optical slice (with a fixed Z coordinate in the XY projection, a fixed Y coordinate in the XZ projection and a fixed X coordinate in the YZ projection [XZ and YZ projections]), or a maximum image of the whole data set (Figure 2a), is displayed. The position of the cursor in the front view (XY projection) determines the Y coordinate of the slice displayed in the XZ projection as well as the X coordinate of the slice displayed in the YZ projection. In the same way the position of the cursor in the other two boxes determines the Z coordinate of the slice displayed in the XY projection. Moving the cursor, the user can 'travel' through the image, obtaining insight into the local features of the image. Tracing a chromosome results in a string of X, Y and Z coordinates. Such a string of coordinates not only reduces the vast amount of data containing a 3D image but also enables a mathematical description and comparison of prophase chromosomes (see below).

In Figure 2b, a reconstruction of the traced chromosome no. 1 of Figure 2a is presented. In this example, the traced chromosome has been copied to an empty image. The new image was then displayed by the SFP algorithm (simulated fluorescence process; van der Voort *et al.* 1989). Note that the thickness of the chromosome is arbitrary.

3D-shape parameters

Curvature and torsion are parameters that are well suited to describe the 3D shape of a curve (Worring *et al.* 1994). Therefore, the positions of local curvature maxima and of an alteration of helical handedness (torsion zero crossing or torsion flip) along the chromosome axes were used as descriptors of chromosome shape. In each of the defined substages of prophase described above, these parameters were used to compare individual chromosomes.

As an example, the curvature pattern and the curve representation of a mid-prophase chromosome are shown in Figure 3. The three-box view (Figure 3a) shows the 3D-coordinate representation displayed by the on-line curve analysis program (Woltring 1986, Worring *et al.* 1994). The square markers on the three projections of the curve indicate the local curvature maxima.

With respect to torsion and torsion sign, it is important to realise that any curve that is not in a plane has positive or negative torsion. That is, it is always a (partly) right- or (partly) left-handed helix. Therefore, the pieces of chromosome bounded by two torsion alternations were tested for being a full helical turn. A curve was defined to be a full helical turn when the total angular deviation of the projection of that curve on a plane perpendicular to the line through the curve boundaries was at least 360°.

Early prophase analysis

In early prophase, individual chromosomes could not be identified, either by stereo imaging or by reconstruction with the cursor program. However, stretches of chromosome strands could be traced and the torsion sign (whether left (−) or right (+)) could be determined. Two chromosome stretches with a full left- and right-handed helical turn are shown in Figure 4a,b. To aid spatial appreciation, the tracings have been displayed with the SFP-algorithm (cf. van der Voort *et al.* 1989). The thickness of coiled stretches was roughly of the order of 500 nm. In Figure 1a, a typical coiled stretch has been indicated by an arrow. No consecutive full helical turns were found in an early prophase chromosome and we could not judge whether left- and right-handed turns occur in one and the same chromosome.

Mid prophase analysis

Typical reconstructed images of mid-prophase chromosomes are shown in Figure 4c. In this figure, one pair of chromosomes no. 1 is depicted according to their original spatial relationship in the cell. On average, these chromosomes had a length of 14.1 ± 4.0 μm. For statistical analysis, 40 mid-prophase chromosomes no. 1 were analysed by estimating the curvature and torsion along the central axes.

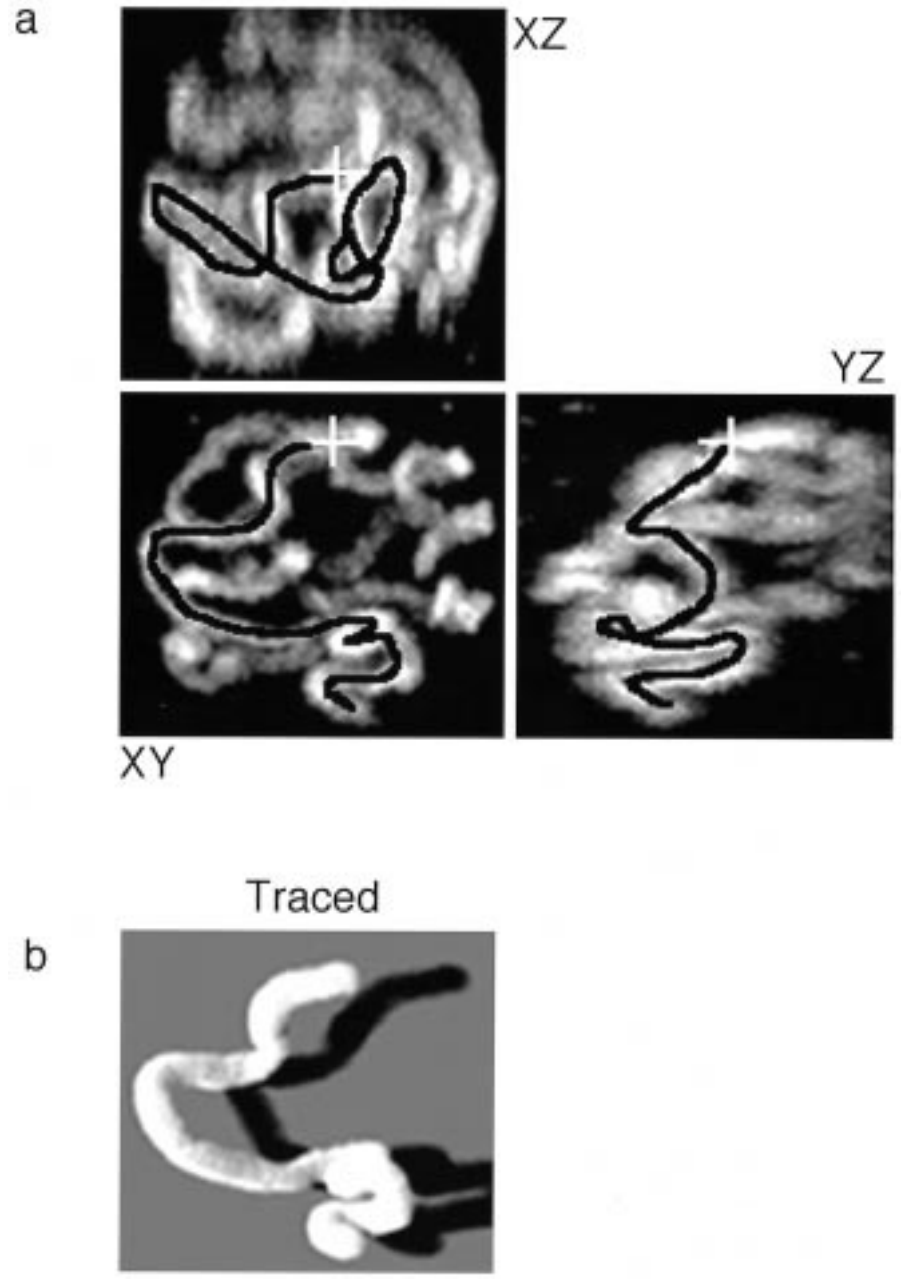

Figure 2. The interactive program including the automated tracing cursor. (**a**) Three projections of a confocal data set displayed in the boxes XY (lower left), XZ (top) and YZ (right). In the XY box a maximum image of the confocal stack is displayed. In the XZ and YZ boxes two cross-sections at the cursor position are displayed. With the 3D cursor displayed in each box, the user interactively indicates a starting position and direction, for instance at a chromosome telomere. After that, the cursor automatically traces the central axis of the chromosome until it is stopped by the user or reaches a user-defined stop position. During tracing, equidistant points along the axis are recorded as 3D Cartesian co-ordinates. Note that the recorded points have subvoxel accuracy. In the left image, the cursor has traced the chromosome. (**b**) To facilitate direct visual inspection of the tracing result, the traced chromosome is copied from the image to the lower box marked 'traced' where it is displayed with the SFP (simulated fluorescence process) algorithm.

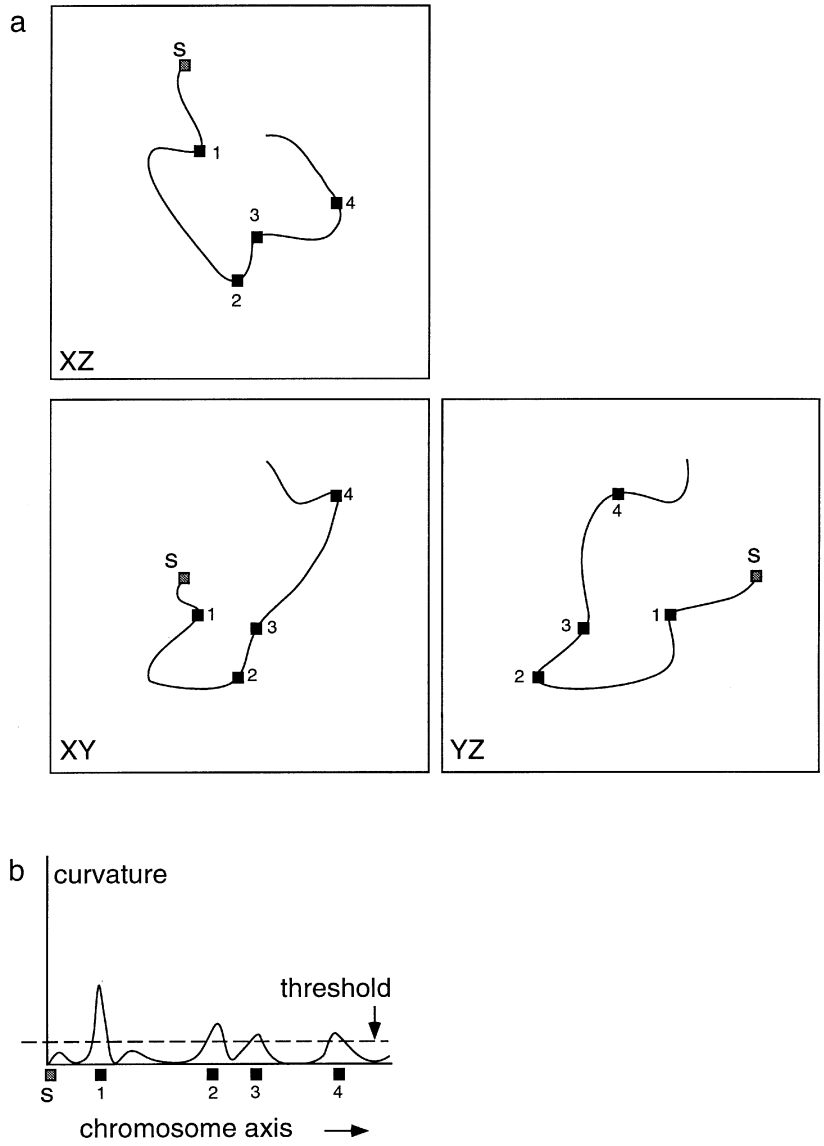

Figure 3. Schematic representation of the interactive curve analysis program. (**a**) A spline fitted to a 3D co-ordinate string obtained from a prophase chromosome is displayed in three views (see Figure 2). (**b**) A graph of the curvature (amount of bending) along the curve (chromosome axis) is displayed. Each local curvature maximum that is greater than a certain threshold (dotted horizontal line) is marked with a dark square corresponding to the dark squares in the curve display. The grey square marked S is the starting position of the tracing.

The local maxima of curvature along each chromosome axis were determined. A frequency histogram of the 99 maxima of 40 mid-prophase chromosomes no. 1 is shown in Figure 5a. It can be seen that the distribution pattern of the maxima is rather uniform.

The torsion alternations along the axes of mid-prophase chromosome no. 1 were also determined and the frequency of their occurrence in ten regions along the chromosome axes was tested by comparing the found distribution with a random distribution. In this case, a uniform distribution of torsion alternations along the axis has been taken as a random distribution. At the 5% significance level, the alternation appeared to be uniformly distributed (data not shown). It also appeared that between torsion alternations the mid-prophase strands did not satisfy the defined conditions for a full helical turn.

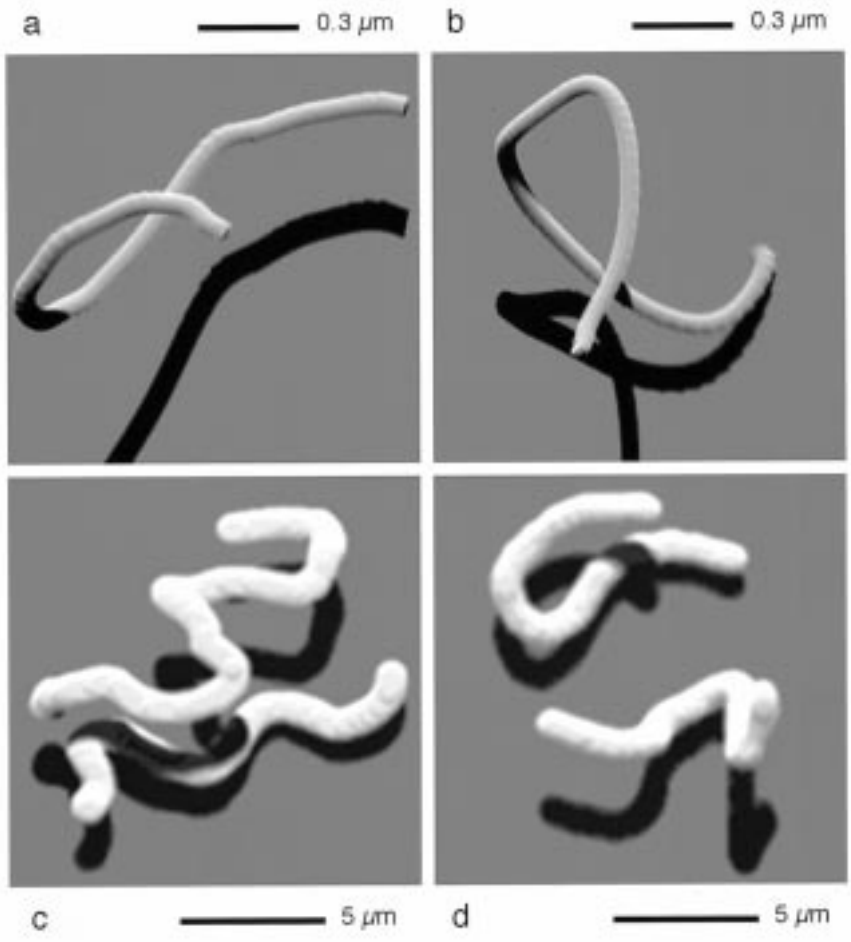

Figure 4. SFP images of reconstructions of two early prophase stretches (**a**, **b**) and two pairs of homologous chromosomes of mid (**c**) and late prophase (**d**). A left- and right-handed helix of an early prophase stretch are shown in (**a**) and (**b**), respectively. A meandering pattern with multiple regions of considerable bending in mid prophase (**c**) and a remaining loop with two regions of considerable bending in late prophase (**d**) can be seen as general features, respectively. The thickness of the reconstructed chromosomes is arbitrary. Note the difference in the scale bars and also note that the early prophase reconstructions refer only to short stretches of a chromosome.

Late prophase analysis

A reconstructed late-prophase chromosome is shown in Figure 4d. On average, late-prophase chromosomes had a length of 9.5 ± 2.1 μm. These chromosomes are not only shorter than mid-prophase ones (Figure 4c; 14.1 ± 4.0 μm), but they also contain fewer bends. The local curvature maxima were determined in 40 late-prophase chromosomes no. 1. From each of the 40 chromosomes, the two highest curvature maxima were taken and plotted in a histogram divided into twelve categories representing twelve successive regions along the chromosome central axis (Figure 5b). In contrast to the situation in mid prophase, here the KS test (Kolmogorov 1933) revealed the presence of a preferential region of high curvature at roughly one third of the chromosome axis ($n = 80$; $d_{max} = 0.13$; $c = 0.12$) indicating that, in the transition from mid to late prophase, the last remaining bends have a defined position.

Discussion

The division of prophase into substages enabled us to establish some features of the dynamics of chromo-

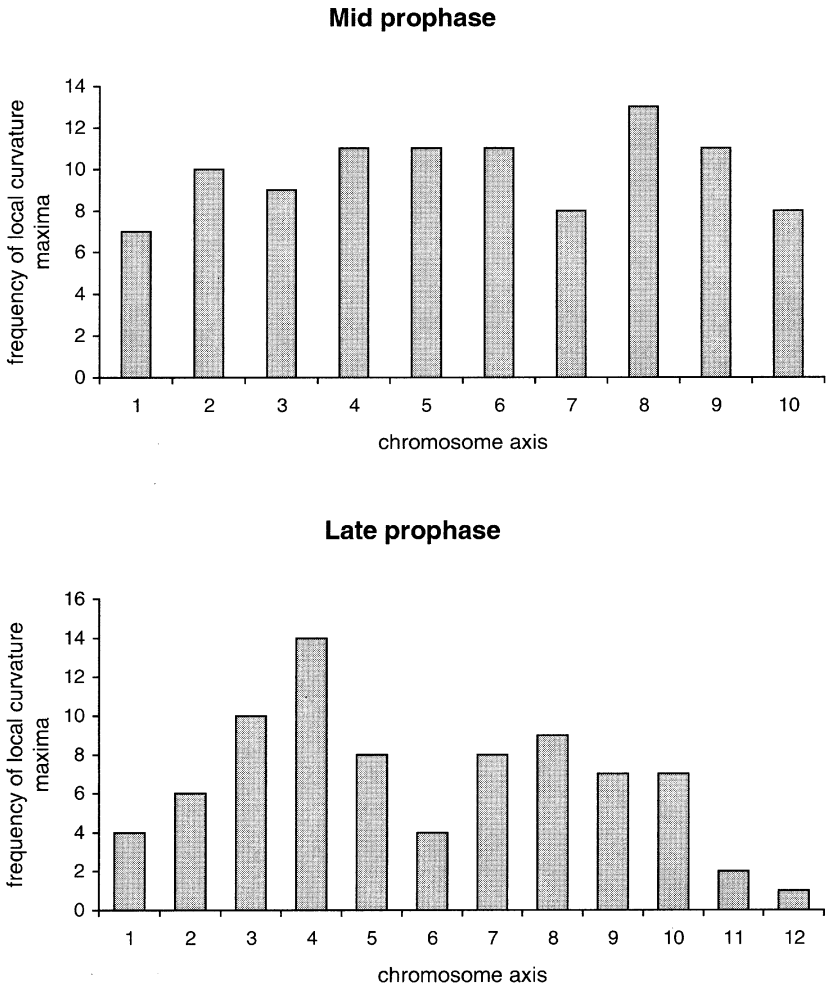

Figure 5. Curvature maxima in mid and late prophase chromosomes. Forty chromosomes no. 1 were represented as strings of 3D co-ordinates. The curvature was calculated along the axes. (**a**) Frequency histogram of curvature local maxima along the mid-prophase chromosome axis. (**b**) Frequency histogram of curvature local maxima along the late-prophase chromosome axis.

some contraction from early to late prophase. In the mid and late prophase substages, a variety of shapes was observed in chromosome no. 1. Yet, as has appeared from the visual representation and from the subsequent statistical comparison, there were global tendencies with respect to the 3D folding. It should be noted that our analysis bears on the spatial course of the geometric chromosomal axis and that chromosomal thickness or surface texture (see Sumner 1990) have not been taken into account. In early prophase nuclei, threads of variable thickness do occur (in contrast to mid and late prophase). The thicker strands might be the result of chromosome compaction towards mid prophase. The early prophase chromosome examples shown in Figure 4a,b refer to short chromosome stretches with a thickness of the order of 500 nm. Our methodology does not allow us to judge whether the partly helical stretches represent sister chromatid pairs or temporarily separated sister chromatids.

Mid prophase

At this stage of mitosis, individual chromosomes could be recognized on the basis of their length. Therefore, a statistical comparison of curvature and torsion along 40 chromosomes no. 1 has been carried out. Curvature maxima appeared to occur along the whole length of the chromosome, in contrast to the situation of late prophase. It should, however, be

emphasized that we could not distinguish between the two telomeres. Thus, a specific curvature feature in one half of the chromosome would have been obscured.

Alternations of helical handedness were observed, though the regions bounded by the torsion alternation points did not satisfy the definition of a full helical turn (see Results). We believe this to be due, at least in part, to the large nucleolus in *C. capillaris* (see Mintijn *et al.* 1999). Presumably, chromosomes are forced to reside in a relatively thin spherical shell, bounded by the nuclear envelope and the nucleolus. Thus full helical turns seem not to be possible, resulting in a meander-like chromosomal bending pattern with torsion alternations occurring at the points where the meander turns. This is schematically depicted in Figure 6a.

Late prophase

In late prophase, chromosome no. 1 often displays one remaining central loop. Statistical analysis of local bending maxima along the chromosome axis supports the idea that late-prophase chromosomes have preferential regions of high bending (Figures 5b & 6b). These preferential regions occur at positions about one third and two thirds along the chromosome. Because these features seem so dominant, the fact that we cannot distinguish between the two telomeres does not appear to be a serious handicap here. The occurrence of high degrees of bending at fixed chromosomal positions is compatible with the results of a 3D time-lapse study of *Drosophila melanogaster* embryonic nuclei (Hiraoka *et al.* 1989). These authors showed that both chromosome decondensation in telophase and condensation in the subsequent prophase take place at the same focal points at the nuclear membrane. More recently, evidence has been presented for *Drosophila* that specific chromosome loci interact with the nuclear envelope during interphase (Marshall *et al.* 1996). One could speculate that such focal points represent points of considerable bending as seen here in late prophase.

Transition between prophase shapes

Models of chromatin/chromosome compaction generally assume a successive ‘superposition’ of folding patterns (see for instance Manuelides 1990), i.e. each level of compaction is maintained when going to a higher level. A general feature appears to be the folding of a nucleosome strand into the so-called 30-nm fibre. Confusion exists about the arrangement of nucleosomes within the 30-nm fibre. However, recent electron cryomicroscopic images strongly suggest the occurrence of a 3D-zigzag folding pattern (Bednar *et al.* 1998). One could speculate that the local left- and right-handed helices detectable in early prophase chromosomes represent coiled 30-nm fibres. Subsequent levels of folding could ultimately lead to late-prophase chromosomes. Although the late-prophase

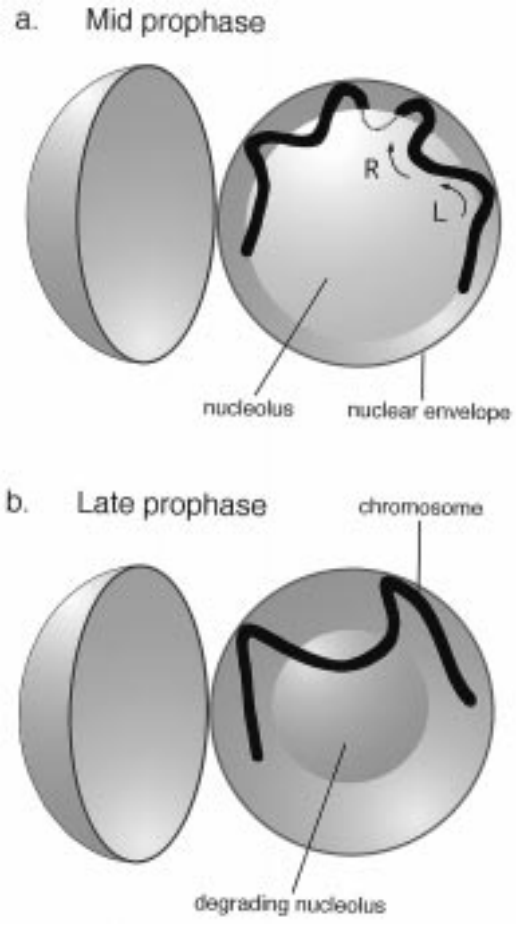

Figure 6. Tentative model for the position of mid- and late-prophase chromosomes in the nucleus. (**a**) The alternations of helical handedness in mid prophase are well explained when it is considered that the basically 2D meander is forced to reside in a spherical shell, i.e. the volume bounded by the large nucleolus and the nuclear membrane. (**b**) In late prophase, two preferential positions of high curvature that appeared from the data (Figure 5) might represent the last attachment points of the chromosome to the nuclear membrane.

chromosomes are clearly shorter than the mid-prophase chromosomes (see above), visual inspection of the confocal images (see Figure 1) shows that they become hardly any thicker. If so, the transition from mid to late prophase seems to be the result of tighter chromatin packing, rather than addition of an extra level of coiling. After immunostaining of topoisomerase II in histone H1-depleted metaphase chromosomes, the sister chromatid pairs showed helical winding of opposite handedness (Boy de la Tour & Laemmli 1988). Perhaps our mid- and late-prophase chromosomes contain two tightly intertwined helices which become dissolved upon entering metaphase.

Our data refer to one particular chromosome (with the exception of early prophase) and one can ask the question whether they also apply to other *C. capillaris* chromosomes. It appears likely that the features described for early and mid prophase do so. In the case of the late-prophase chromosome, we found a reproducible shape. The centromeric region in chromosome no. 1 is about one quarter of the chromosome length from the nearest telomere (Oud *et al.* 1989). This indicates that one of the regions of considerable bending, about one third and two thirds along the chromosome axis, is not related to the position of the centromere. Thus, the possibility should be considered that physical rather than chemical factors are involved in shaping a late-prophase chromosome.

Acknowledgements

We thank Mark Savenije for his expert technical assistance in 3D-image presentation.

References

Agard DA, Sedat JW (1983) Three-dimensional architecture of a polytene nucleus. *Nature* **302**: 676–681.

Bednar J, Horowitz RA, Grigoryev SA *et al.* (1998) Nucleosomes, linker DNA, and linker histone form a unique structural motif that directs the higher-order folding and compaction of chromatin. *Proc Natl Acad Sci USA* **95**: 14173–14178.

Belmont AS, Braunfeld MB, Sedat JW, Agard DA (1989) Large-scale chromatin structural domains within mitotic and interphase chromosomes in vivo and in vitro. *Chromosoma* **98**: 129–143.

Boy de la Tour E, Laemmli UK (1988) The metaphase scaffold is helically folded: sister chromatids have predominantly opposite helical handedness. *Cell* **55**: 937–944.

Brakenhoff GJ, van der Voort HTM, Oud JL (1990) Three-dimensional image representation in confocal microscopy. In: Wilson T ed. *Confocal Microscopy.* London: Academic Press, pp 185–197.

DuPraw EJ (1966) Evidence for a folded fibre organization in human chromosomes. *Nature* **209**: 577–581.

Earnshaw WC (1988) Mitotic chromosome structure. *BioEssays* **9**: 147–150.

Hiraoka Y, Minden JS, Swedlow JR, Sedat JW, Agard DA (1989) Focal points for condensation and decondensation revealed by three dimensional *in vivo* time-lapse microscopy. *Nature* **342**: 293–296.

Hochstrasser M, Sedat JW (1987) Three dimensional organization of *Drosophila melanogaster* interphase nuclei. I. Tissue-specific aspects of polytene nuclear architecture. *J Cell Biol* **104**: 1455–1470.

Houtsmuller AB, Smeulders AWM, van der Voort HTM, Oud JL, Nanninga N (1993) The homing cursor; a tool for three dimensional chromosome analysis. *Cytometry* **14**: 501–509.

Kolmogorov A (1933) Sulla determinazione empirica di una legge di distribuzione. *G Ist Ital Attuari* **4**: 83–91.

Luger K, Mäder AW, Richmond RK, Sargent DF, Richmond TJ (1997) Crystal structure of the nucleosome core particle at 2.8 A resolution. *Nature* **389**: 251–260.

Manuelidis L (1990) A view of interphase chromosomes. *Science* **250**: 1533–1540.

Manuelidis L, Chen TL (1990) A unified model of eukaryotic chromosomes. *Cytometry* **11**: 8–25.

Marshall WF, Dernburg AB, Harmon B, Agard DA, Sedat JW (1996) Specific interactions of chromatin with the nuclear envelope: positional determination within the nucleus in *Drosophila melanogaster*. *Mol Biol Cell* **7**: 825–842.

Montijn MB, Houtsmuller AB, ten Hoopen R, Oud JL, Nanninga N (1999) The 5S rRNA gene clusters have a defined orientation toward the nucleolus in *Petunia hybrida* and *Crepis capillaris*. *Chromosome Res* **7**: 387–399.

Oud JL, Mans A, Brakenhoff GJ, van der Voort HTM, van Spronsen EA, Nanninga N (1989) Three-dimensional chromosome arrangement of *Crepis capillaris* in mitotic prophase and anaphase as studied by confocal scanning laser microscopy. *J Cell Sci* **92**: 329–339.

Sedat JW, Manuelidis L (1977) A direct approach to the structure of eukaryotic chromosomes. *Cold Spring Harbor Symp Quant Biol* **42**: 331–350.

Sumner AT (1990) Scanning electron microscopy of mammalian chromosomes from prophase to telophase. *Chromosoma* **100**: 410–418.

van der Voort HTM, Brakenhoff GJ, Baarslag MW (1989) Three-dimensional visualization methods for confocal microscopy. *J Microsc* **153**: 123–132.

Woltring HJ (1986) A Fortran package for generalized cross-validatory spline smoothing and differentiation. *Adv Eng Software* **8**: 104–113.

Worring M, Pfluger P, Smeulders AWM, Houtsmuller AB (1994) Measurement of 3-D line shaped objects. *Pat Rec Lett* **15**: 497–506.